Quaternary Science Reviews 98 (2014) 74–83

Contents lists available at ScienceDirect

Quaternary Science Reviews

journal homepage: www.elsevier.com/locate/quascirev

Slow retreat of a land based sector of the West Greenland Ice Sheet during the Holocene Thermal Maximum: evidence from threshold lakes at Paakitsoq

Lena Håkansson [a, b, *], Jason P. Briner [c], Camilla S. Andresen [a], Elizabeth K. Thomas [d], Ole Bennike [a]

[a] Department of Marine Geology and Glaciology, Geological Survey of Denmark and Greenland, Øster Voldgade 10, DK-1350 Copenhagen K, Denmark
[b] Department of Geology and Mineral Resources Engineering, Norwegian University of Science and Technology, Sem Særlands Veg 1, N-7491 Trondheim, Norway
[c] Department of Geology, University at Buffalo, Buffalo, NY 14260, USA
[d] Department of Geological Sciences, Brown University, Providence, RI 02912, USA

ARTICLE INFO

Article history:
Received 24 October 2013
Received in revised form
15 May 2014
Accepted 20 May 2014
Available online

Keywords:
Greenland Ice Sheet
Holocene Thermal Maximum
Neoglaciation
Little Ice Age
Paleoclimate

ABSTRACT

Records from two connected proglacial threshold lakes at Paakitsoq, west Greenland have been analyzed in order to investigate the response of a land-based ice sheet margin to Holocene climate change. The results are used to test whether or not the land terminating margin at Paakitsoq behaved synchronously with the nearby marine terminating Jakobshavn Isbræ during the Holocene. The radiocarbon dated lake sediment cores indicate that the ice margin retreated to its present position ~6.5 ka ago and thereafter maintained a relatively stable configuration similar to the present for >1000 years, despite summer temperatures >2 °C higher than today. The lakes became non-glacial after 5.4 cal. ka BP, when the ice margin retreated behind a drainage divide situated ~1.5 km inland of the present margin. By this time, Jakobshavn Isbræ had already reached its minimum configuration. The Paakitsoq ice margin remained >1.5 km inland of its present margin until after 240 ± 20 cal. yr BP; after this time, both Paakitsoq ice margin and Jakobshavn Isbræ reached their Holocene maxima during the later stage of the Little Ice Age. Our results suggest that the present ice margin position at Paakitsoq is relatively stable in a warming climate but after a total retreat of ~1.5 km behind the present margin position it may become marine based and more unstable due to marine melting and calving processes.

1. Introduction

Reconstructions of past climate variability and ice sheet changes place constraints on climate sensitivity of ice sheets and provide important data for forecasting the impacts of future warming on sea level changes. Changes of the Greenland Ice Sheet (GIS) are of broad importance due to the influence of melt water on global sea level rise and potentially on large-scale ocean circulation and thus the global climate system in general (e.g. Alley et al., 2005, 2010; IPCC, 2007). Recent instrumental data show that the periphery of the GIS is thinning rapidly and that this thinning is greater around marine terminating outlet glaciers than at neighboring regions with slower moving ice (Sole et al., 2008). However, instrumental data only record changes during the last century. In contrast, geological reconstructions provide insights about ice margin behavior on longer time scales and are therefore important for the understanding of the sensitivity of the GIS to climate change.

Paleoclimate reconstructions suggest that peak Holocene warmth (the Holocene Thermal Maximum) in Greenland was reached between 9 and 3 ka, depending on which temperature proxy is considered (Fredskild, 1973; Wagner et al., 2000; Kaplan et al., 2002; Kaufman et al., 2004; Young et al., 2011; Axford et al., 2013). Further, modeling of borehole temperatures from the GRIP ice core site shows that temperatures in Greenland were higher than today between 8 and 5 ka, Dahl-Jensen et al., 1998). This warming triggered a large portion of the western GIS to retreat behind its present day position (Weidick et al., 1990, 2012; Weidick and Bennike, 2007; Briner et al., 2010; Young et al., 2011). However,

* Corresponding author. Department of Geology and Mineral Resources Engineering, Norwegian University of Science and Technology, Sem Særlands Veg 1, N-7491 Trondheim, Norway. +46 704 809038.
E-mail address: lena.hakansson@geol.lu.se (L. Håkansson).

http://dx.doi.org/10.1016/j.quascirev.2014.05.016
0277-3791/

it remains a challenge to estimate the total amount of retreat between regional deglaciation and the Neoglacial readvance of the ice margin as most of the geological evidence of the smaller-than-present ice configuration is currently beneath the modern ice sheet. Constraints on the timing of mid-Holocene retreat can be provided by investigations of proglacial threshold lakes (Kaplan et al., 2002; Briner et al., 2010, 2011; Larsen et al., 2011; Young et al., 2011; Kelley et al., 2012). When the ice margin advances into the catchment of a lake, rock flour from glacial erosion is washed into the lake and results in deposition of minerogenic sediment. Once the ice margin retreats out of the catchment, deposition in the lake will change from minerogenic to organic-rich.

The objective of this study is to investigate the response of the land-based ice sheet margin at Paakitsoq, western Greenland, to Holocene climate change by analyzing records from two connected proglacial threshold lakes. We compare our findings with similar studies from nearby Jakobshavn Isbræ (Briner et al., 2010, 2011; Young et al., 2011), which is one of the most productive outlets of the GIS, in order to investigate the relationship between a large outlet glacier and a nearby land based ice margin. This provides insights into both the timing and magnitude of land and marine terminating margin responses to past climate variability.

2. Setting

The present day margin of the GIS at Paakitsoq, western Greenland, is situated near the head of the Paakitsup Ilorlia fjord, 25 km east of Disko Bugt and ~30 km north of Jakobshavn Isbræ (Fig. 1a). The distance between the head of the fjord and the ice margin is ~10 km and the landscape is characterized by ice scoured terrain with crystalline bedrock. Neoglacial moraines reach ~50 m above the surroundings and confine a 500 m wide zone of stagnant, sediment covered ice fronting the GIS margin. Maps of the subglacial topography near the study site reveal a drainage divide located at ~250 m above sea level and ~1.5 km inland of the present day ice margin; farther inland the terrain slopes towards a >200 m deep trough (Ahlstrøm et al., 2008; Mottram et al., 2009; Gogineni, 2012).

We investigated two lakes at Paakitsoq, Lake Lo and Lake 187 (informal names, Figs. 1b and 2), which are both situated at 187 m asl. Lake 187 is partly ice dammed and therefore has a

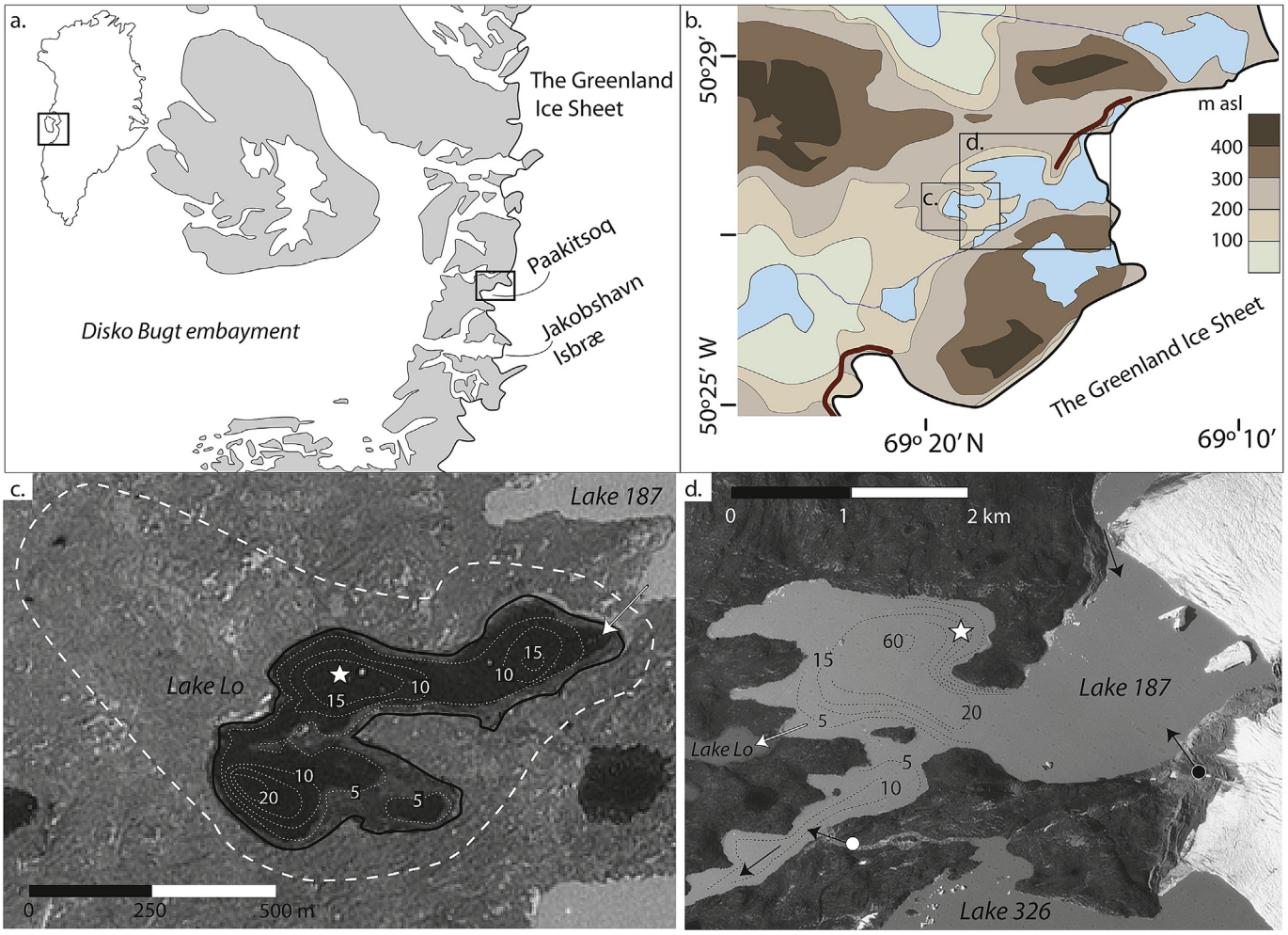

Fig. 1. (a) Map of the Disko Bugt region with an inset map of Greenland. The frame marks the location of the study area. (b) Location of the study lakes and the 2010 ice sheet margin. The red line marks the Neoglacial moraine and the topography is shown with 100 m contour intervals. (c) Aerial photograph from 1959 showing Lake Lo. The catchment area is shown with a white dashed line and the white arrow marks the episodic inflow from Lake 187 to Lake Lo. The white star marks the core site for cores 10-Lo-2A and -2B. (d) Lake 187 is shown on an aerial photograph from 1982. The arrow marked with a white circle shows the pre-1989 drainage of Lake 326 into Lake 187 and the arrow with a black circle mark the post-1989 drainage according to Thomsen and Olesen (1990). The black and white dotted lines show lake bathymetry in meters, arrows show inflow/outflow streams and the white star mark core site for core 10-L187-1A. (For interpretation of the references to color in this figure legend, the reader is referred to the web version of this article.)

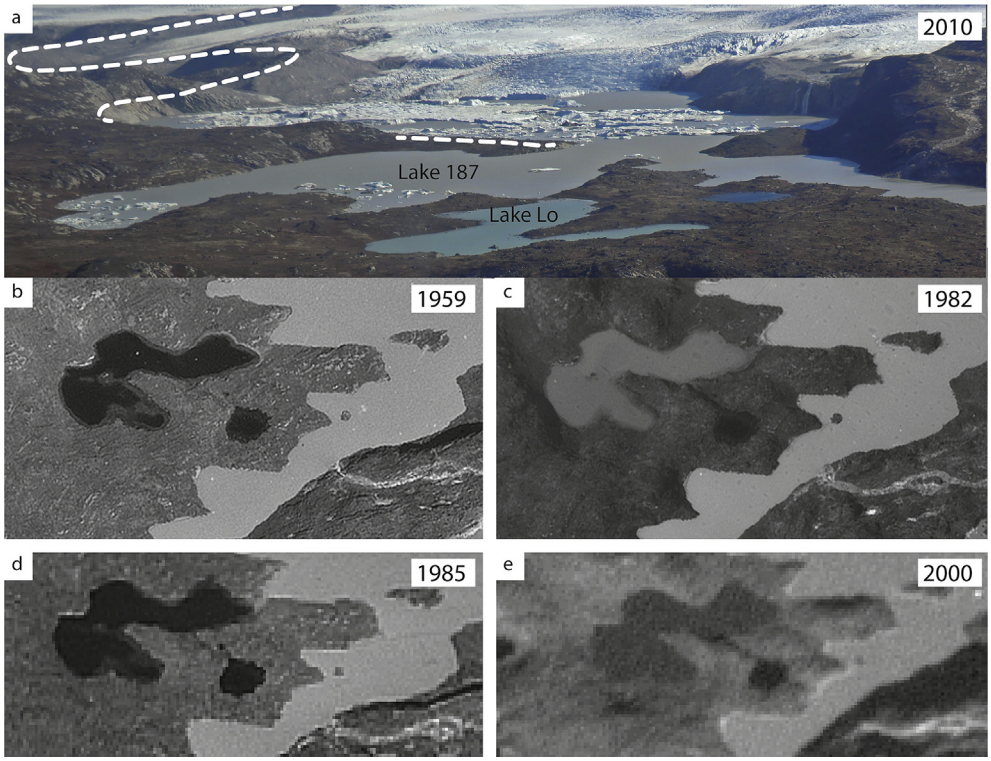

Fig. 2. Images showing changes of the study lakes between 1959 and 2010 AD. Silty water conditions in Lake Lo indicate that there is an inflow of meltwater from the ice sheet through Lake 187. On the 2010 photograph of the ice sheet margin at Paakitsoq and the study lakes, the crest of the Neoglacial moraine is marked with a dashed white line. The images labeled 1959–1985 AD are aerial photographs and the image labeled 2000 AD is a Landsat TM.

varying water level controlled by the position of the ice margin and seasonal melting. When ice retreats behind the drainage divide 1.5 km inland it no longer delivers meltwater to Lake 187. The threshold between Lake 187 and Lake Lo is shallow and narrow, which makes Lake Lo sensitive to small changes in the water level of Lake 187.

2.1. Lake Lo

Lake Lo (69° 28′N, 50° 17′W; 187 m asl) has a surface area of ~0.2 km^2. The lake has no outflow and the only inflow is episodic and occurs from Lake 187, across a shallow threshold that separates Lake Lo and Lake 187 (Fig. 1c). Flow of water from Lake 187 to Lake Lo depends on both ice damming of Lake 187 and sufficient meltwater flux to elevate the level of Lake 187. In the summer 2010 the water level of Lake 187 was high, which resulted in inflow of silt-laden melt water across the threshold (Fig. 2a). Landsat images show that this was also the case in 2000 AD, and perhaps since 2000 AD (Fig. 2e). Aerial photographs from 1959 to 1985 AD show clear water conditions in Lake Lo, but in the summer of 1982 the lake water was silty (Fig. 2). The catchment area is 0.9 km^2 during times of no inflow, with gentle slopes towards the lake (Fig. 1c).

2.2. Lake 187

Lake 187 (69°28′N, 50°17′W; 187 m asl) has a surface area of ~2.7 km^2 and an ice-dammed sub-basin of ~1 km^2 that is in contact with the ice sheet. The ice-dammed basin is situated inboard of a Neoglacial moraine (Fig. 1d). The catchment of Lake 187 is mostly glacial and the discharge into the basin depends not only on the topography of the glacier bed, but also on glacier surface and englacial drainage. Run-off conditions have been modeled in order to investigate the potential of the area for hydropower and the glacial drainage basin has been estimated to be 100–160 km^2 (Ahlstrøm et al., 2008). At present the lake receives inflow directly from the ice margin and from a river that runs parallel to the Neoglacial moraine, which drains a proglacial lake 2.5 km to the north. Lake 187 also receives inflow to its southern part from an ice-dammed lake to the south (Lake 326, Fig. 1d). Before 1989 AD this drainage flowed over a bedrock threshold at the NW corner of Lake 326, a drainage path that had been stable for >41 years. However, retreat of the ice margin caused Lake 326 to drain, which resulted in a lake level lowering of 14 m and a re-routed drainage along the ice margin to the SE corner of Lake 187 (Thomsen and Olesen, 1990). The main outflow of Lake 187 is in the SW corner of the lake (Fig. 1d).

3. Methods

3.1. Coring

In August 2010, sediment cores were retrieved from Lake Lo and Lake 187. The coring sites were selected after bathymetrical surveys using a Garmin GPSMAP 400 series GPS receiver. Lake Lo has three different sub-basins with maximum depths of ~20, 16 and 15 m (Fig. 1c). Two sediment cores with intact sediment/water interfaces were collected from the central 16 m deep basin using a Universal Coring system (10-Lo-2A and 10-Lo-2B, Fig. 1c). Core 10-Lo-2A is 93 cm and 10-Lo-2B is 96 cm long. Bathymetrical surveys of Lake 187 showed a large central basin >60 m deep with gentle slopes and a flat bottom (Fig. 1d). Bathymetry also revealed a sill at 20 m depth between the central basin and the ice marginal sub-basin and another sill separating the outflow from the rest of the lake at 1.5 m depth (Fig. 1d). A 1.5 m long core was collected from the gentle north slope of the central basin at 14 m water depth using a piston/percussion coring system mounted on a raft (10-L187-1A, Fig. 1d).

Table 1
Radiocarbon ages from the lake sediment cores.

Core no	Depth (cm)	Dated material	Radiocarbon age (years BP)	Calibrated age (years BP)	Laboratory no
10-Lo-2A	10.5	Bulk	815 ± 50	724 ± 43	LuS 9286
10-Lo-2A	12.5–14.5	*Sphagnum* sp.[a]	605 ± 50	593 ± 46	LuS 9629
10-Lo-2A	37.5–39.5	*Empetrum nigrum*[a]	3440 ± 60	3694 ± 80	LuS 9724
10-Lo-2A	39.5	Bulk	3405 ± 50	3649 ± 63	LuS 9725
10-Lo-2	50–52	*Betula nana*[a]	4680 ± 65	5411 ± 89	LuS 9723
10-Lo-2A	51.8	Bulk	4905 ± 50	5630 ± 42	LuS 9287
10-Lo-2A	65.5	Bulk	5835 ± 55	6645 ± 64	LuS 9722
10-Lo-2A	87.0	Bulk	5655 ± 55	6429 ± 59	LuS 9719
10-Lo-2A	85–87	*Warnstorfia exannulata*[b]	5635 ± 55	6409 ± 57	LuS 9720
10-Lo-2B	52.0	*Scorpidium scorpioides*[b]	5740 ± 55	6527 ± 73	LuS 9630
10-L187-1A	150.0	Peat	550 ± 50	554 ± 39	LuS 9288

[a] Terrestrial macrofossils.
[b] Aquatic moss.

3.2. Chronology

Samples of organic material were picked, wet sieved, and dried at the Geological Survey of Denmark and Greenland (GEUS) and submitted for radiocarbon dating using Accelerator Mass Spectrometry (AMS) at Lund University. Terrestrial plant remains, aquatic mosses and humic acid extracts from bulk sediment samples were dated (Table 1). The lakes in the study area are surrounded by Precambrian crystalline bedrock and are expected to have no hard water effect. However, in the Arctic a low rate of plant decomposition may result in a high abundance of radiocarbon depleted organic material in soils, which in turn may be deposited in lakes (Abbott and Stafford, 1996). Therefore radiocarbon ages from bulk sediment samples are potentially older than their deposition age. To assess the potential presence of radiocarbon depleted organic material, pairs of macrofossil and bulk sediment samples were dated from four levels from core 10-Lo-2A. Radiocarbon ages were calibrated and an age-depth model developed using clam software in the open source statistical environment R and the IntCal09 calibration curve (Reimer et al., 2009; Blaauw, 2010;; R Development Core Team, 2010).

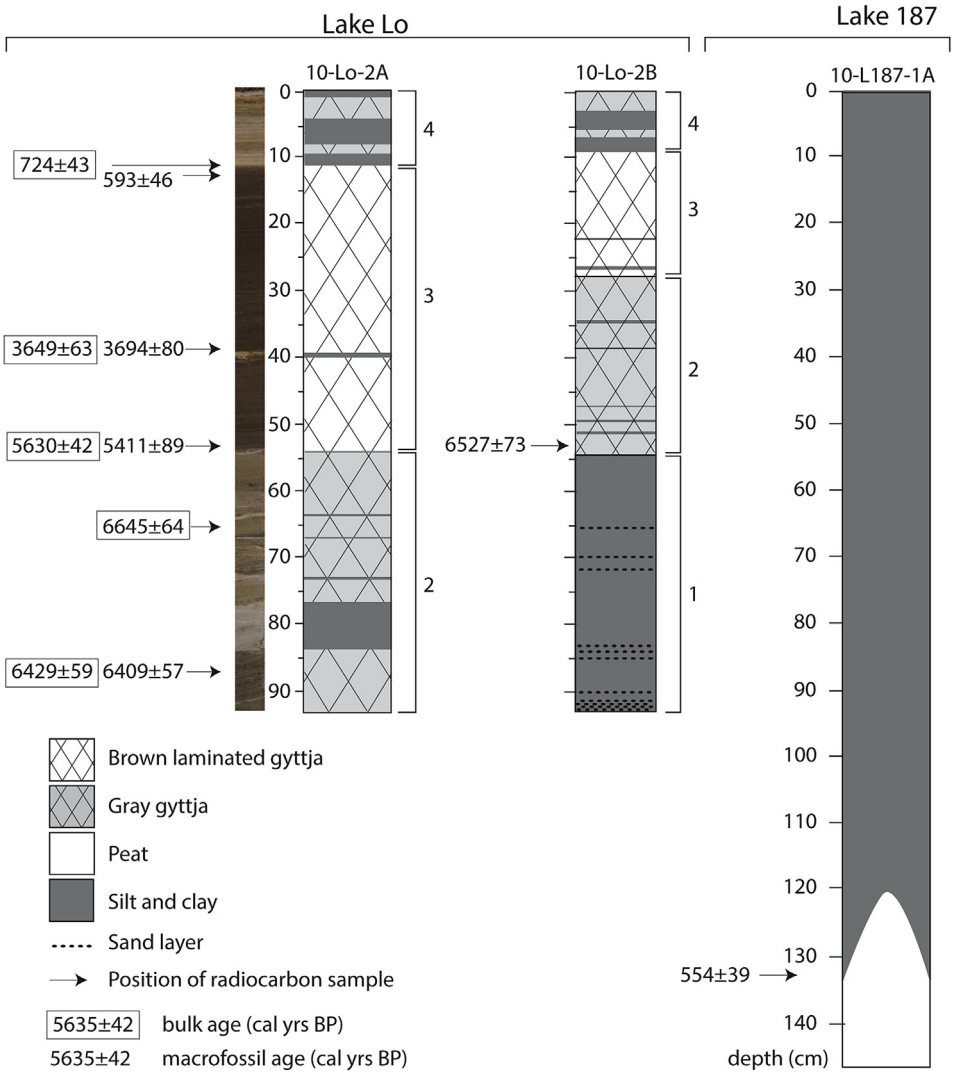

Fig. 3. Lithostratigraphy of cores from Lake Lo (cores 10-Lo-2A and -2B taken from 16 m water depth) and Lake 187 (core 10-L187-1A taken from 14 m water depth). The sampling depths of radiocarbon ages are marked with arrows.

3.3. Physical and geochemical properties

Physical and geochemical properties were measured in core 10-Lo-2A. Density scanning was carried out at GEUS using gamma ray logging. This provides relative density changes in the core. Organic matter content was determined by percentage loss-on-ignition (LOI) at 550 °C and measured in 5–10 mm intervals down the core. Magnetic susceptibility (MS) was measured continuously at 5 mm intervals on the split core surfaces using a Bartington magnetic susceptibility meter with a hand held MS2E sensor. Fe and Ti were measured through X-ray Fluorescence (XRF) by using the Avaatech core scanner at The Royal Netherlands Institute for Sea Research. XRF core-scanning measurements were obtained directly at the split-core surface at 1 mm intervals with generator settings of 10 kV and a sampling time of 20 s and the data are presented as peak areas of counts per second (cps).

4. Results

4.1. Lake Lo

4.1.1. Lithostratigraphy

The Lake Lo succession was divided into four units based on sediment cores 10-Lo-2A and 10-Lo-2B (Fig. 3), which show similar stratigraphies. Units 1–4, from bottom to top, are: (1) laminated silt and clay with sand layers, (2) gray gyttja with silt layers, (3) laminated brown gyttja, and (4) silt and clay interlayered with gyttja (Fig. 3).

In 10-Lo-2A, Unit 2 spans from 92 to 52 cm; however, the lower boundary of Unit 2 is not present in this core. The lower 9 cm consist of dark gray gyttja rich in aquatic mosses. Between 83 and 77 cm there is a weakly laminated silt layer, overlain by gray gyttja with mm-thick silt layers, one of which occurs at the upper boundary of this unit. Unit 3, from 52 to 10.5 cm, is composed of brown laminated gyttja with a sharp lower boundary. Thin bands of small black granules occur between 49.5 and 40 cm. A white silt layer (0.5 cm thick) is present at a depth of 39.5 cm with a transitional lower, and a sharp orange-colored upper, boundary. Unit 4 spans from 10.5 cm to the surface. This unit has a sharp lower boundary to Unit 3 and consists of three minerogenic layers interlayered with gyttja. The two lower minerogenic layers consist of laminated silt and clay and are 3 and 2.5 cm thick, respectively, and are interlayered with gray gyttja.. The uppermost 3 cm of the core consists of a soft and uncompacted, orange-gray gyttja topped-off by a 3 mm thick, massive silt layer on top.

In core 10-Lo-2B, Unit 1 spans from 94 to 57 cm. The lowermost part of this core consists of laminated silt and clay with fining-upwards sand layers. The sand layers are thicker in the lowermost part of Unit 1. The upper half of this core (57–0 cm) shows the same general stratigraphy as core 10-Lo-2A.

4.1.2. Chronology

From core 10-Lo-2A, three radiocarbon ages are from terrestrial plant macrofossils, one age is from aquatic moss and five ages are from bulk-sediment samples. Four pairs of macrofossil and bulk-sediment samples come from approximately the same depths (Table 1). The samples between 13 and 10.5 cm indicate that the bulk sediment sample is at least 130 years older than the macrofossil sample. At 87, 51.8 and 39.5 cm ages from bulk sediment samples are only ~20–40 years older than macrofossil ages. One bulk-sediment sample from 65.5 cm yielded an age older than the underlying bulk-macrofossil pair and has therefore been excluded from the age-depth model. One basal age from aquatic moss in core 10-Lo-2B yielded an age of 6527 ± 73 cal. yr BP (Table 1). The ages show that the sedimentation rates in core 10-Lo-2A were highest in Units 2 (0.35 mm/yr) and 4 (0.32 mm/yr), and lowest in Unit 3 (0.08 mm/yr, Fig. 4).

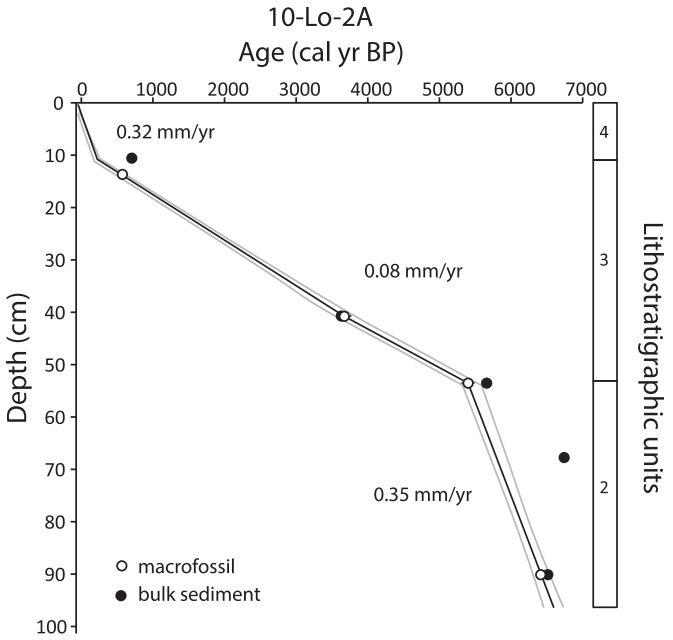

Fig. 4. The age-depth model for core 10-Lo-2A was developed using clam software in the open-source statistical environment R and the IntCal09 calibration curve (Reimer et al., 2009; Blaauw, 2010; R Development Core Team, 2010). Lithostratigraphic units are presented in the right panel and sedimentation rates (mm/yr) are shown for each unit.

Because of variable offsets between bulk and macrofossil ages at different depths, only macrofossil ages were used to develop the age-depth model for core 10-Lo-2A. The different lithological units are assumed to show different depositional rates, and therefore, an age-depth model was obtained for Unit 3 by linear interpolation between the three macrofossil-based radiocarbon ages from this unit, and extrapolated to the contact with Unit 4 (Table 2). The ^{14}C-dated macrofossil sample from the base of Unit 3 (at 51.8 cm) is used as the age of the contact between Units 2 and 3 (Table 2). The one-sigma age ranges of the contacts were then used to create the final age-model, with linear interpolation between the calibrated macrofossil ages, the surface of the core, and the contact between Units 3 and 4 (Fig. 4). According to the age-depth model, the basal age of core 10-Lo-2A is 6560 ± 70 cal. yr BP and further discussion is based on the following age ranges from the age-depth model for the lithological units (Table 2): 6.6–5.4 ka (Unit 2), 5.4–0.24 ka (Unit 3) and 0.24–0 ka (Unit 4).

4.1.3. Physical and geochemical properties

Physical and geochemical data are shown in Fig. 5. Generally, LOI is lowest in the minerogenic layers (<3%), slightly higher in the gray gyttja of Units 2 and 4 (4.5–10%) and highest in the brown gyttja of

Table 2
Data used in the clam software to develop the age-depth model for 10-Lo-2A.

Data type	Depth (cm)	^{14}C age[a]	YBP	Age error (yr, 1σ)
Surface	0		−60	5
Interpolated (Unit 3–4)	11.5		360[b]	35
Terrestrial macrofossil	13.5	605		50
Terrestrial macrofossil	39.5	3440		60
Terrestrial macrofossil	51.8	4680		65
Interpolated (Unit 2–3)	53		5549[b]	90
Aquatic moss	87	5635		55

[a] Clam software calibrates radiocarbon ages automatically before calculating the age model.
[b] Ages for gyttja-silt contacts obtained with a linear age-depth model for Unit 3 using the three macrofossil ages therein.

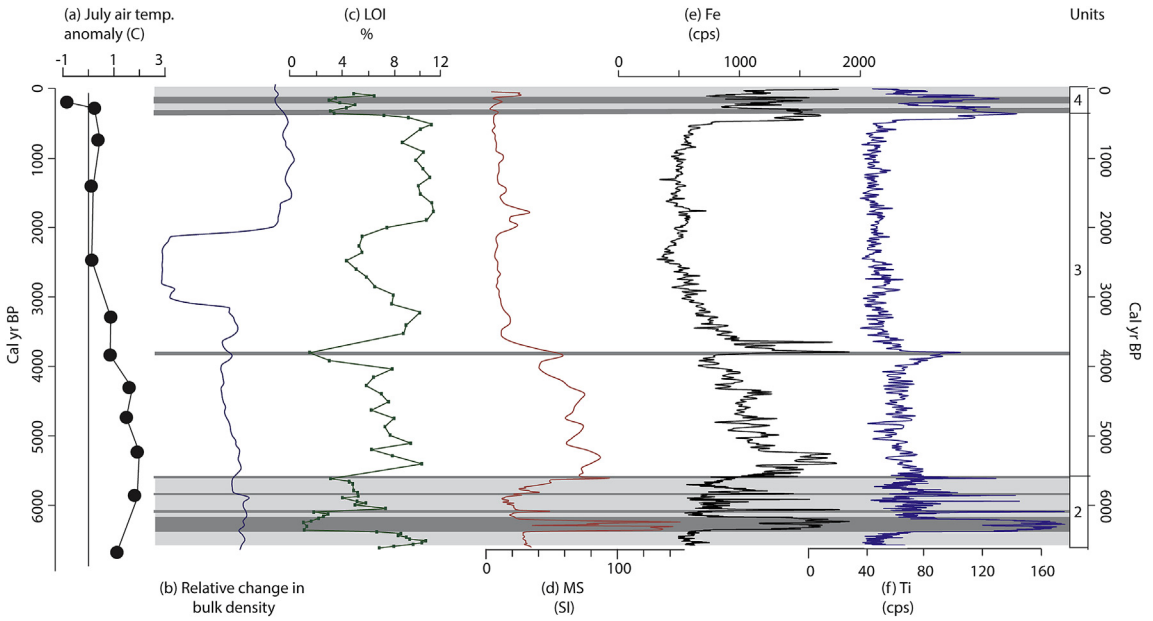

Fig. 5. Geochemical and physical data from core 10-Lo-2A plotted against age The light gray shading in the background illustrates gray gyttja facies, the dark gray illustrates minerogenic layers and white marks non-glacial sedimentation. Lithostratigraphic units are shown to the far right in the figure. (a) Chironomid inferred July temperature anomaly from a lake near Jakobshavn Isfjord (Axford et al., 2013). (b) Relative change in bulk density through the core derived from gamma ray logging. (c) Loss-on-ignition (LOI). (d) Magnetic susceptibility (MS) measured with a hand held MS2E sensor at 5 mm intervals. (e) Fe and (f) Ti derived from XRF scanning with 1 mm resolution.

Unit 3 (6–11%). However, there is a drop in the LOI-curve in the brown gyttja between 2.8 and 2.1 ka with values <4.5%. This interval with low LOI coincides with a drop in the relative bulk density. Both below and above this interval the bulk density is relatively constant only slightly higher in the upper compared to the lower part (Fig. 5b). In Units 2 and 4 the MS-curve shows an inverse correlation to LOI, but in Unit 3 there are two intervals (5.4–3.5 ka and 2.1–1.6 ka) which exhibit relatively high values both in LOI and MS (Fig. 5c and d). The MS tracks the Fe data throughout the core, however, the Fe data have a higher resolution (5 mm and 1 mm, respectively). Ti counts show close correspondence with the lithology, with peaks recording each silt layer, and low and relatively constant values through the organic-rich sediment intervals (Fig. 5f). In Unit 3 average Ti counts are slightly higher below and slightly lower above the thin silt layer at 3.8 ka (c. 65 and 50 cps, respectively).

4.2. Lake 187

4.2.1. Lithostratigraphy and chronology

The sediment sequence in Lake 187 was investigated in core 10-L187-1A (Fig. 3). The lower unit in this core consists of peat consisting of rootlets (150–130 cm). The transition between peat and minerogenic sediments (133–110 cm) was deformed during coring. Silty clay with sand-rich layers is found on top of the deformed transition between 110 and 70 cm. The uppermost 70 cm of this core consists of compact clayey silt. A sample for radiocarbon dating was taken 4 cm below the upper boundary of the peat and gave an age of 550 ± 40 cal. yr BP.

5. Interpretation

5.1. The Lake Lo record

In the brown gyttja of Unit 3 the anomalously low organic matter content as indicated by the drop in LOI values between 2.8 and 2.1 ka coincide with a drop in the relative bulk density and it is therefore suggested that the sedimentation rate during this interval was higher relative to the rest of Unit 3. The drop in LOI is interpreted as an artifact of the higher sedimentation rate during this interval and it is therefore suggested that the organic matter deposition was relatively constant throughout the brown gyttja.

MS is the degree of magnetization of a material in response to an applied magnetic field and thus positive MS values indicate the presence of minerals containing iron. The source of iron and titanium in the Lake Lo sediments is from the surrounding crystalline bedrock. Fe-oxides within the sediments can either be primary, originating directly from minerals in the surrounding bedrock or alternatively secondary oxides produced by iron-oxidizing bacteria within the lake. In contrast, Ti-oxides cannot be produced within the lake and thus the changes in Ti in the Lake Lo core is used as an indicator of detrital input. There are two intervals within the brown gyttja where high MS and Fe values coincide with low Ti and high LOI: one in the lowermost and another in the upper part of Unit 3 (between 5.4–3.5 ka and 2.1–1.6 ka, respectively, Fig. 5). Because the high Fe counts coincide with relatively low Ti, it is suggested that iron oxides were produced within the lake indicating limited mixing in the lake at this time (Emerson et al., 2010). The limited mixing may have been be triggered by the isolation of the lake basin and by decreasing windiness caused by the retreat of the ice margin away from the Lake's catchment.

6. Ice margin history inferred from lake sediment sequences

Lakes in West Greenland without glacial or fluvial input are typically dominated by deposition of brown or olive green gyttja with a relatively high content of organic matter (LOI ~5–30%) whereas glacial lakes are characterized by deposition of silt, clay and sand, which are often laminated, with low organic matter content, below ~5% (e.g. Briner et al., 2010; Young et al., 2011; Wagner and Bennike, 2012). Minerogenic sediment may have accumulated in Lake Lo in three ways: (1) during deglaciation when the ice margin was in the Lake Lo catchment, (2) when the ice margin had a configuration similar to the present causing damming

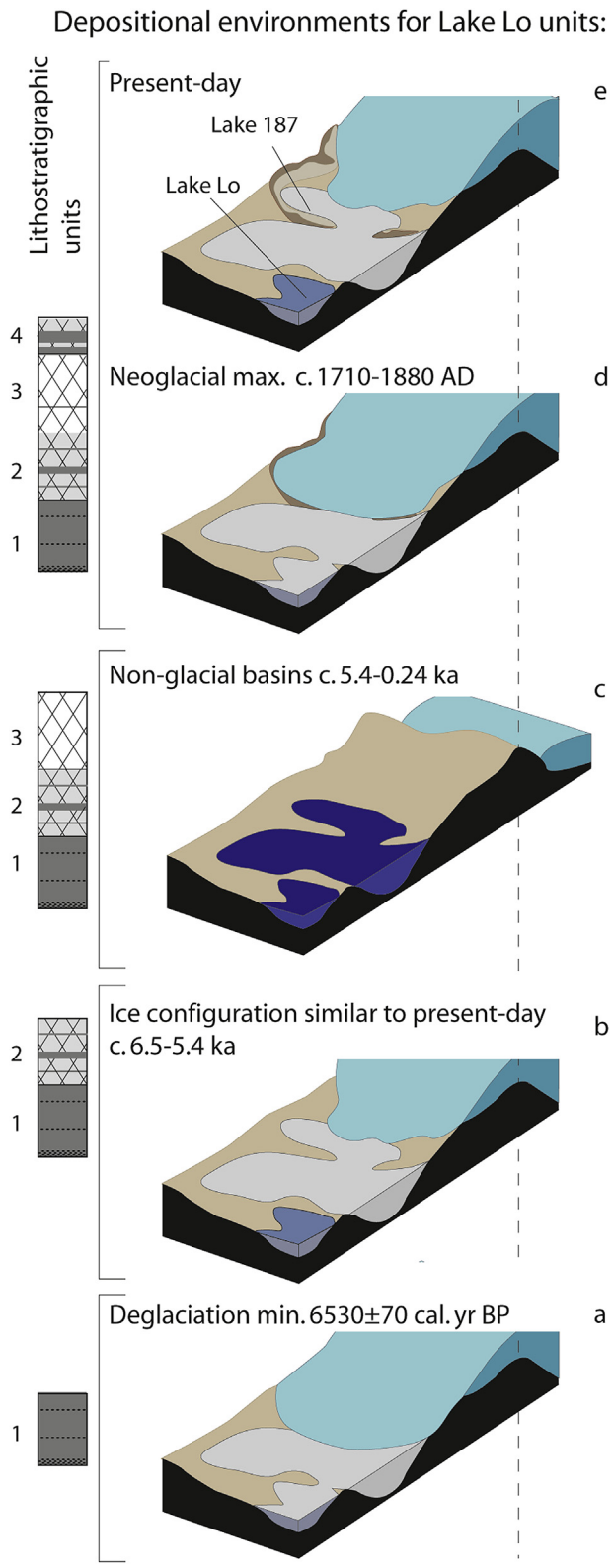

Fig. 6. Schematic diagrams of the study area, illustrating changes in the study lakes and the GIS margin. The depositional environments of Lake Lo lithostratigraphic units are shown. The position of the drainage divide, ~1.5 km behind the present ice margin, is marked with a vertical dashed line; when the ice margin retreated behind this point the investigated lakes switched from glacial to non-glacial basins. (a) During deglaciation silt and clay with sand layers were deposited in Lake Lo (Unit 1). (b) The ice margin is situated close to its present-day position and gray gyttja with silt layers is deposited in Lake Lo (Unit 2). (c) The ice margin retreated behind the drainage divide and the lakes were non-glacial basins. Brown laminated gyttja was deposited in Lake Lo and the water level of Lake 187 was at least 14 m lower than at present (Unit 3). (d) The ice margin advanced into the lakes' catchments and reached its maximum Neoglacial position; at this position silt and clay was deposited in both lakes (silt layers in Unit 4). (e) The ice margin is close to its present position and gray gyttja is deposited (gyttja layers in Unit 4). (For interpretation of the references to color in this figure legend, the reader is referred to the web version of this article.)

of Lake 187 and overflow of silt-laden meltwater into Lake Lo, or (3) when Lake Lo was isolated from Lake 187, by paraglacial reworking of old glacial sediments from the catchment slopes (Ballantyne, 2002; Rubensdotter and Rosqvist, 2009; Bakke et al., 2010). The ice margin history at Paakitsoq was inferred from the investigated lake records and the changes in the studied lakes and in the GIS margin is illustrated in Fig. 6.

6.1. Regional deglaciation, min. 6527 ± 73 cal. yr BP

The minerogenic sediments of Unit 1 are interpreted as having been deposited directly following the deglaciation of the basin (Figs. 3 and 6a). Upward fining sand layers probably represent turbidity flows, which may have been deposited while the ice margin was still in the Lake Lo catchment, or perhaps very soon after. Above the deglacial mud is a sequence of organic-rich sediments (Fig. 3) with a basal age of 6527 ± 73 cal. yr BP which put minimum constraints on the timing of the deglaciation of the Lake Lo basin.

6.2. Ice configuration similar to present day (6.5–5.4 ka)

The organic-rich sediments comprise gray gyttja with silt layers (Unit 2) and brown laminated gyttja (Unit 3). The gray color, the generally lower LOI and the slightly higher Ti values in Unit 2 indicate slightly higher minerogenic content in comparison to Unit 3. Unit 2 also has a significantly higher average sedimentation rate (0.35 mm/yr) compared to Unit 3 (0.08 mm/yr). The minerogenic component and the higher sedimentation rate of Unit 2 may be interpreted in at least two ways: (i) the sediment is partly glacial in origin, requiring that the ice sheet margin resided within the catchment of Lake 187 (and spilling meltwater into Lake Lo) at the time of deposition or (ii) the minerogenic content originates from paraglacial reworking of glacial sediment mantling catchment slopes. We favor the first interpretation because Unit 2 is similar, both in appearance (Fig. 3) and in MS and Ti values (Fig. 5), to the sediments which have been deposited during the last century in the upper part of Unit 4. This interpretation is also supported by the fact that Lake Lo has a small and low-relief catchment area (Fig 1c). With such a small catchment it is difficult to explain the continuous input of minerogenic sediment lasting ~1 ka as paraglacial reworking of old glacial sediments. Furthermore, the upper contact of Unit 2 is sharp, which is characteristic for shifts between glacial and non-glacial conditions in proglacial threshold lakes (Kaplan et al., 2002; Briner et al., 2010). Thus, we interpret Unit 2 as having been deposited when the ice margin reached and then maintained a configuration similar to that of the present day with Lake 187 being partly ice dammed, enabling inflow to Lake Lo over the threshold between the lakes (Fig. 6b).

6.3. Non-glacial conditions (5.4–0.24 ka)

The onset of brown gyttja deposition around 5.4 ka (Unit 3, Table 2) is interpreted as a shift from glacial to non-glacial conditions, indicating that at this time the GIS margin had retreated behind the drainage divide situated ~1.5 km inland of the present margin (Fig. 6c). During non-glacial conditions Lake Lo has no inflow stream and the only inflow is through run-off from the small catchment. This isolation of the basin may have led to anoxic

conditions in the lake and the formation of iron oxides. The retreat of the ice margin behind the drainage divide may also have led to less windy conditions at the lakes leading to decreased mixing.

The thin silt layer in the middle of the Unit 3 was deposited around 3.8 ka and may either represent a short-lived advance of ice across the drainage divide or an erosion event within the catchment. We consider that a readvance of the ice margin into the drainage basin at 3.8 ka is less likely based on radiocarbon ages of marine shells found in Neoglacial moraines adjacent to the Paakitsoq ice margin. These shells give ages ranging between 4.6 and 3.1 ka which suggests that during the time of deposition of the silt layer in Lake Lo the ice margin was situated at least 10 km inland of its present position, a distance given by the eastward extent of a deep subglacial trough found east of the drainage divide (Fig. 7, Weidick and Bennike, 2007). Therefore, the preferred interpretation is that the minerogenic input to the basin originates from within the catchment. The presence of peat at the 10-L187-1 core site at 14 m water depth constrains the maximum water level in Lake 187 during the non-glacial conditions (Figs. 1d and 3).

6.4. The Neoglaciation (AD 1710–1880)

Unit 4 comprises three layers of silt and clay interlayered with silty gyttja (the lower two minerogenic layers are cm-thick and laminated and the upper layer is only a few mm thick). We interpret these lithologies as being deposited when the ice sheet margin was within the catchment of the lakes (Figs. 3 and 6d, e). The minerogenic layers were probably deposited when the ice sheet margin was at or close to the Neoglacial maximum, and layers of silty gyttja formed when the ice margin had retreated to a position similar to at present, more distal to the lakes. The age of the boundary between Units 3 and 4 of 240 ± 20 cal. yrs BP (1710 ± 20 AD) provides a maximum limiting age for the first Neoglacial advance of the ice sheet margin into the catchment and for the onset of minerogenic deposition (Table 2). Furthermore, a maximum age constraint on the first ice occupation of the surrounding catchment come from radiocarbon dating of peat from Lake 187 providing an age of 550 ± 40 cal. yrs BP (1400 ± 40 AD). The dated peat sample is taken a few cm below the upper boundary and therefore we consider the 240 ± 20 cal. yrs BP age from the age-depth model to more precisely constrain the Neoglacial advance into the lake basins. We infer that the middle minerogenic layer of Unit 4 (Fig. 3) was formed during the Little Ice Age maximum: historical documentation from the Paakitsoq region shows that the ice margin was still advancing around 1850 AD (Rink, 1857), and reached its maximum Neoglacial position around 1880 AD (Hammer, 1889; Weidick and Bennike, 2007). Gray gyttja was deposited in Lake Lo after the final retreat from the 1880 AD position. Landsat images show that the water in Lake Lo has been silty since 2000 AD (Fig. 2e) and that there has been an inflow of glacial meltwater from Lake 187. The thin silt layer in the top of Unit 4 may have been deposited during this interval of increased silt input to Lake Lo, which could be a response to increased melting caused by rapid warming during the last decade.

7. The relationship between the ice margin at Paakitsoq and Jakobshavn Isbræ

Lake Lo was deglaciated by ~6.5 ka as indicated by the basal age of the radiocarbon dated sediment cores. We use this age to constrain when the ice margin at Paakitsoq reached its present-day position. At Jakobshavn Isbræ the present ice margin position was reached almost 1 ka earlier as indicated by basal radiocarbon ages and ^{10}Be ages from areas near the margin of Jakobshavn Isbræ (~7.3 ka BP, Briner et al., 2010; Young et al., 2011). Furthermore, ^{10}Be ages from a locality close to the present ice margin half way between the Paakitsoq ice margin and Jakobshavn Isbræ, suggest deglaciation by 7.6 ka BP (Corbett et al., 2011).

Following deglaciation, the marine terminating margin of Jakobshavn Isbræ continued a steady retreat towards its minimum configuration, which is thought to have been reached between 6 and 5 ka ago (Weidick and Bennike, 2007; Briner et al., 2010). In contrast, our results show that the lakes at Paakitsoq were proglacial (represented by Units 1 and 2 in the Lake Lo record) until ~5.4 cal. ka BP (Fig. 6). This implies that ice resided in the catchment of the lakes for >1000 years (6.5–5.4 ka). This can be interpreted in at least two ways: the GIS margin at Paakitsoq was either (i) stable in a configuration similar to that of the present day until ~5.4 ka, or (ii) retreating at a steady rate, but leaving behind a local ice cap

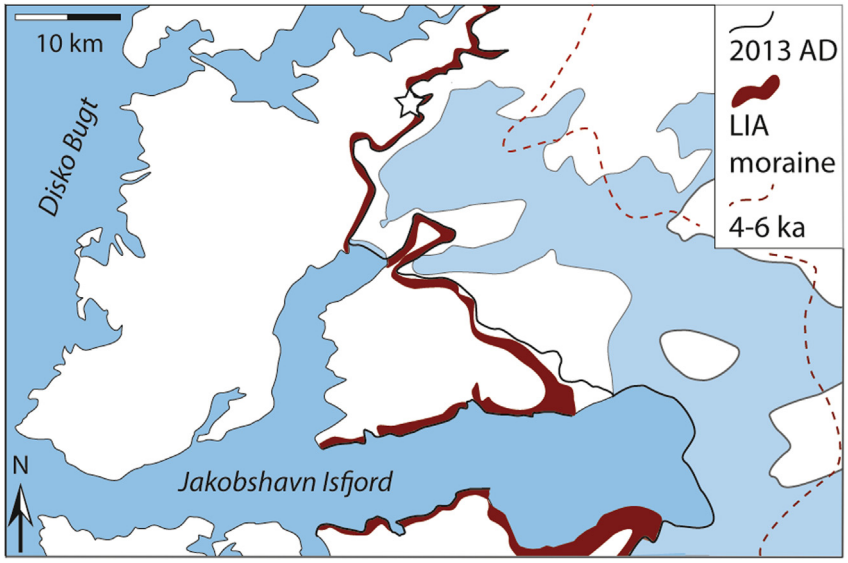

Fig. 7. Generalized subglacial bed topography showing areas above (white) and below (blue) the present sea level. The black line represents the ice sheet margin in 2013 and the red dashed line shows the reconstructed minimum position of the ice margin during the Holocene, after Weidick and Bennike (2007). The map covers the bed topography for the area from Jakobshavn Isbræ in the south (after CReSIS data, Gogineni, 2012) to the Paakitsoq ice margin in the north (after Mottram et al., 2009). The white star marks the location of the studied lakes. (For interpretation of the references to color in this figure legend, the reader is referred to the web version of this article.)

which resided at the drainage divide and delivered melt water into the catchment of the lakes until 5.4 ka BP. It is not possible to distinguish between these scenarios from the lake records alone, what they show is simply a signal of the presence or absence of glacial ice in the lake catchment. However, the Paakitsoq drainage divide is situated at <300 m asl, which is far below the modern equilibrium line altitude (ELA) located presently above 1000 m asl. In addition, the ice sheet margin retreated to its present-day position during a time when mean summer air temperatures in the Disko Bugt region were higher than at present (2–3 °C higher between 6 and 4 ka, Young et al., 2011; Axford et al., 2013). The present rate of down-wasting at the Paakitsoq margin is 3.5 m/yr and during warmer conditions even higher rates are expected (Ahlstrøm et al., 2008). Altogether, the survival of a local ice cap in the catchment of the studied lakes for >1000 years is unlikely. Hence we suggest that the land terminating Paakitsoq ice margin was stable in a configuration similar to the present, and no more than ~1.5 km inland of its present terminus, until 5.4 cal. ka BP.

Constraints on the timing of the minimum configuration of the ice sheet margin are provided by radiocarbon ages of marine fossils incorporated in Neoglacial moraines. The occurrence of shells indicates that when the ice sheet was at its minimum position, marine water inundated troughs that today are located beneath the ice sheet. Ages range between 6.1 and 3.4 cal. ka BP from the Paakitsoq ice margin (Weidick et al., 1990; Weidick and Bennike, 2007). The presence of fjords presently covered by the land terminating ice margin revealed in sub-ice topography maps suggests that the ice margin retreated 15–20 km east of its present position during the middle Holocene (Weidick et al., 1990; Weidick, 1992).

Based on proglacial lake records it has been suggested that the Jakobshavn Isbræ ice margin was at its minimum configuration between 6 and 5 ka (Briner et al., 2010). A slightly later timing is suggested by the oldest radiocarbon ages from marine fossils in Neoglacial moraines to around 5–3 ka (Briner et al., 2014). By the time Jakobshavn Isbræ reached its minimum Holocene position, the Paakitsoq ice margin was still in a configuration similar to the present as suggested by our results. This asynchronous retreat history is likely due to the different processes of ablation that operate at land versus marine terminating ice margins. In particular, calving and submarine melting at the ice front in deep embayments can lead to rapid ice mass loss and ice margin retreat (Pfeffer, 2007; Holland et al., 2008; Nick et al., 2009; Rignot et al., 2010; Straneo et al., 2010; Vieli and Nick, 2011; Andresen et al., 2012). In contrast, the retreat of the Paakitsoq ice sheet margin behind the drainage divide was land-based and therefore caused predominantly by surface melt. By combining sub-ice topography data from the Jakobshavn Isbræ region (from CReSIS, Gogineni, 2012) with sub-ice topography data from Paakitsoq (Mottram et al., 2009), we see that the subglacial trough east of the study site probably was connected with the Disko Bugt embayment only via the Jakobshavn trough (Fig. 7). If indeed this is the only pathway for marine water into the fjord behind the present ice margin at Paakitsoq, then this connection was open at least between 4.6 and 3.1 cal. ka BP, which is the time period spanned by the radiocarbon dated marine shells from the Neoglacial moraines at Paakitsoq. However, it should be noted that only four shells have been dated so far.

8. Implications for future warming

A local temperature record infer warmer-than-present temperatures by at least 7.1 ka and that Holocene peak warmth in the Jakobshavn Isbræ region occurred between 6 and 4 ka with summer temperatures 2–3 °C warmer than present (Axford et al., 2013). Our results suggest that the ice sheet margin at Paakitsoq was stable in a configuration similar to the present for >1 ka despite warmer-than-present summers. The mid-Holocene represents a period of climate conditions not all that different from today, however, there are some fundamental differences. CO_2 concentrations in the atmosphere increased during the mid-Holocene, just like today. However, it needs to be emphasized that this increase was more than three orders of magnitude smaller compared to the last 160 yr period and was likely a response to, rather than a forcing of, climate change (Indermühle et al., 1999). Furthermore, orbital parameters differed from today; the Holocene Thermal Maximum is commonly associated with the summer insolation maximum in the north (Wanner et al., 2008; Bartlein et al., 2011). Because of these differences in the climatic boundary conditions our reconstructions of the mid-Holocene retreat of the Paakitsoq ice margin cannot be used as a direct analog to how this section of the west Greenland Ice Sheet may react to projected future warming. In any case, our results suggest that once the Paakitsoq ice margin retreats ~1.5 km behind the present margin position, the ice terminus will reach a point where the terrain drops below the present sea level. Provided a synchronous retreat of Jakobshavn Isbræ allows marine water to intrude into the trough, this may result in increased retreat rates due to marine melt and calving from a marine based ice terminus.

9. Conclusions

Records from two proglacial-threshold lakes fed by the Paakitsoq ice margin (Lake Lo and Lake 187) provide information regarding the ice margin position during the middle and late Holocene.

- A radiocarbon age of basal organic sediment from a sediment core from Lake Lo provides a minimum age for the local deglaciation of 6.5 cal. ka BP. Following deglaciation, the ice margin at Paakitsoq resided near the lake catchments for >1 ka despite inferred mean summer temperatures 2–3 °C higher than present at that time.
- The GIS margin at Paakitsoq retreated inland of its present-day position after 5.4 cal. ka BP and the ice margin probably reached a minimum configuration between 4.6 and 3.1 ka BP.
- The Neoglacial maximum was reached after 1400 AD and probably as late as 1710 AD and lasted until 1880 AD when the ice margin started retreating.
- Our results suggest that the present ice margin position at Paakitsoq is relatively stable in a warming climate but after a total retreat of ~1.5 km behind the present ice margin position it may become more unstable due to marine melting and calving processes as a marine-based ice terminus.

Acknowledgments

This research was funded by the Swedish Research council and SSAG. Nicolás Young and Stefan Truex are acknowledged for help with the coring. John Boserup at GEUS is thanked for helping with laboratory equipment. We acknowledge the use of data from CReSIS generated with support from NSF grant ANT-0424589 and NASA (100000104) grant NNX10AT68G.

References

Abbott, M.B., Stafford Jr., T.W., 1996. Radiocarbon geochemistry of modern and ancient Arctic lake systems, Baffin Island, Canada. Quat. Res. 45, 300–311.
Ahlstrøm, A.P., Mottram, R.H., Nielsen, C.S., Reeh, N., Andersen, S.B., 2008. Evaluation of the future hydropower potential at Paakitsoq, Ilulissat, West Greenland: technical report. Dan. og Grønl. Geol. Unders. Rapp. 38.
Alley, R.B., Clark, P.U., Huybrechts, P., Joughin, I., 2005. Ice-sheet and sea level changes. Science 310, 456–460.
Alley, R.B., Andrews, J.T., Brigham-Grette, J., Clarke, G.K.C., Cuffey, K.M., Fitzpatrick, J.J., Funder, S., Marshall, S.J., Miller, G.H., Mitrovica, J.X., Muhs, D.R.,

Otto-Bliesner, B.L., Polyak, L., White, J.W.C., 2010. History of the Greenland Ice Sheet: paleoclimatic insights. Quat. Sci. Rev. 29, 1728–1756.
Andresen, C.S., Straneo, F., Ribergaard, M.H., Bjørk, A.A., Andersen, T.J., Kuijpers, A., Nørgaard-Pedersen, N., Kjær, K.H., Schjøth, F., Weckström, K., Ahlstrøm, A.P., 2012. Rapid response of Helheim Glacier in Greenland to climate variability over the past century. Nat. Geosci. 5, 37–41.
Axford, Y., Losee, S., Briner, J.P., Francis, D.R., Langdon, P.G., Walker, I.R., 2013. Holocene temperature history at the western Greenland Ice Sheet margin reconstructed from lake sediments. Quat. Sci. Rev. 59, 87–100.
Bakke, J., Dahl, S.O., Paasch, O., Simonsen, J.R., Kvisvik, B., Bakke, K., Nesje, A., 2010. A complete record of Holocene glacier variability at Austre Okstindbreen, northern Norway: an integrated approach. Quat. Sci. Rev. 29, 1246–1262.
Ballantyne, C., 2002. Paraglacial geomorphology. Quat. Sci. Rev. 21, 1935–2017.
Bartlein, P.J., Harrison, S.P., Brewer, S., Connor, S., Davis, B.A.S., Gajewski, K., Guiot, J., Harrison-Prentice, T.I., Henderson, A., Peyron, O., Prentice, I.C., Scholze, M., Seppä, H., Shuman, B., Sugita, S., Thompson, R.S., Viau, A.E., Williams, J., Wu, H., 2011. Pollen-based continental climate reconstructions at 6 and 21 ka: a global synthesis. Clim. Dyn. 37 (3), 775–802.
Blaauw, M., 2010. Methods and code for 'classical' age-modelling of radiocarbon sequences. Quat. Geochronol. 5, 512–518.
Briner, J.P., Stewart, H.A.M., Young, N.E., Phillips, W., Losee, S., 2010. Using proglacial-threshold lakes to constrain fluctuations of the Jakobshavn Isbræ ice margin, west Greenland, during the Holocene. Quat. Sci. Rev. 29, 3861–3874.
Briner, J.P., Young, N.E., Thomas, E.K., Stewart, H.A.M., Losee, S., Truex, S., 2011. Varve and radiocarbon dating support the rapid advance of Jakobshavn Isbræ during the Little Ice Age. Quat. Sci. Rev. 30, 2476–2486.
Briner, J.P., Kaufmann, D.S., Bennike, O., Kosnik, M.A., 2014. Amino acid ratios in reworked marine bivalve shells constrain Greenland Ice Sheet history during the Holocene. Geology 42, 75–78.
Corbett, L.B., Young, N.E., Bierman, P.R., Briner, J.P., Neuman, T.A., Rood, D.H., Graly, J.A., 2011. Paired bedrock and boulder ^{10}Be concentrations resulting from early Holocene ice retreat near Jakobshavn Isfjord, western Greenland. Quat. Sci. Rev. 30, 1739–1749.
Dahl-Jensen, D., Mosegaard, K., Gundestrup, N., Clow, G.D., Johnsen, S.J., Hansen, A.W., Balling, N., 1998. Past temperatures directly from the Greenland Ice Sheet. Science 282, 268–271.
Emerson, D., Fleming, E.J., McBeth, J.M., 2010. Iron-oxidizing bacteria: an environmental and genomic perspective. Annu. Rev. Microbiol. 64, 561–583.
Fredskild, B., 1973. Studies in the vegetational history of Greenland. Medd. Om. Grønl. 198, 1–245.
Gogineni, P., 2012. CReSIS Jakobshavn_2008_2012_composite data. Digital Media, Lawrence, Kansas, USA. http://data.cresis.ku.edu/.
Hammer, R.R.J., 1889. Undersøgelse af Grønlands Vestkyst fra 68°2′ til 70° N.B. Medd. Om. Grønl. 8, 1–32.
Holland, D., Thomas, R.H., de Young, B., Ribergaard, M.H., Lyberth, B., 2008. Acceleration of Jakobshavn Isbrae triggered by warm subsurface ocean waters. Nat. Geosci. 1, 659–664.
Indermühle, A., Stocker, T.F., Joos, F., Fischer, H., Smith, H.J., Wahlen, M., Deck, B., Mastroianni, D., Tschumi, J., Blunier, T., Meyer, R., Stauffer, B., 1999. Holocene carbon-cycle dynamics based on CO_2 trapped in ice at Taylor Dome, Antarctica. Nature 398, 121–126.
IPCC, 2007. Climate change 2007: the physical science basis. In: Soloman, S., Qin, D., Manning, M., Chen, Z., Marquis, M., Averyt, K.B., Tignor, M., Miller, H.L. (Eds.), Contribution of Working Group 1 to the Fourth Assessment Report of the Intergovernmental Panel of Climate Change. Cambridge University Press, Cambridge, 996 pp.
Kaplan, M.R., Wolfe, A.P., Miller, G.H., 2002. Holocene environmental variability in southern Greenland inferred from lake sediments. Quat. Res. 58, 149–159.
Kaufman, D.S., Ager, T.A., Anderson, N.J., Anderson, P.M., Andrews, J.T., Bartlein, P.J., Brubaker, L.B., Coats, L.L., Cwynar, L.C., Duvall, M.L., Dyke, A.S., Edwards, M.E., Eisner, W.R., Gajewski, K., Geirsdottir, A., Hu, F.S., Jennings, A.E., Kaplan, M.R., Kerwin, M.N., Lozhkin, A.V., MacDonald, G.M., Miller, G.H., Mock, C.J., Oswald, W.W., Otto-Bliesner, B.L., Porinchu, D.F., Ruhland, K., Smol, J.P., Steig, E.J., Wolfe, B.B., 2004. Holocene Thermal maximum in the western Arctic (0–180°W). Quat. Sci. Rev. 23, 529–560.
Kelley, S.E., Briner, J.P., Young, N.E., Babonis, G.S., Csatho, B., 2012. Maximum late Holocene extent of the western Greenland Ice Sheet during the late 20th century. Quat. Sci. Rev. 56, 89–98.
Larsen, N.K., Kjær, K.H., Olsen, J., Funder, S., Kjeldsen, K.K., Nørgaard-Pedersen, N., 2011. Restricted impact of Holocene climate variations on the southern Greenland Ice Sheet. Quat. Sci. Rev. 30, 3171–3180.
Mottram, R., Nielsen, C., Ahlstrom, A., Reeh, N., Kristensen, S.S., Christensen, E.L., Forsberg, R., Stenseng, L., 2009. A new regional high resolution map of basal and surface topography for the Greenland ice-sheet margin at Paakitsoq, West Greenland. Ann. Glaciol. 50, 105–111.
Nick, F.M., Vieli, A., Howat, I.M., Joughin, I., 2009. Large-scale changes in Greenland outlet glacier dynamics triggered at the terminus. Nat. Geosci. 2, 110–114.
Pfeffer, W.T., 2007. A simple mechanism for irreversible tidewater glacier retreat. J. Geophys. Res. 112, F03S25.
R Development Core Team, 2010. R: a Language and Environment for Statistical Computing. R Foundation for Statistical Computing, Vienna, Austria. ISBN 3-900051-07-0. http://www.R-project.org (accessed 01.02.10.).
Reimer, P.J., Baillie, M.G.L., Bard, E., Bayliss, A., Beck, J.W., Blackwell, P.G., Bronk Ramsey, C., Buck, C.E., Burr, G.S., Edwards, R.L., Friedrich, M., Grootes, P.M., Guilderson, T.P., Hajdas, I., Heaton, T.J., Hogg, A.G., Hughen, K.A., Kaiser, K.F., Kromer, B., McCormac, F.G., Manning, S.W., Reimer, R.W., Richards, D.A., Southon, J.R., Talamo, S., Turney, C.S.M., van der Plicht, J., Weyhenmeyer, C.E., 2009. IntCal09 and Marine09 radiocarbon age calibration curves, 0–50,000 years cal BP. Radiocarbon 51, 1111–1150.
Rignot, E., Koppes, M., Velicogna, I., 2010. Rapid submarine melting of the calving faces of West Greenland glaciers. Nat. Geosci. 3, 187–191.
Rink, H.J., 1857. Grønland, geografisk og statistisk beskrevet, 1: Det nordre Inspectorat, 420 pp., 2: Det søndre Inspectorat, 588 pp. Andreas Fredrik Høst, Copenhagen.
Rubensdotter, L., Rosqvist, G., 2009. Influence of geomorphological setting, fluvial-, glaciofluvial- and mass-movement processes on sedimentation in alpine lakes. Holocene 19, 665–678.
Sole, A., Payne, T., Bamber, J., Nienow, P., Krabill, W., 2008. Testing hypotheses of the cause of peripheral thinning of the Greenland Ice Sheet: is land-terminating ice thinning at anomalously high rates? The Cryosphere 2, 205–218.
Straneo, F., Hamilton, G.S., Sutherland, D.A., Stearns, L.A., Davidson, F., Hammill, M.O., Stenson, G.B., Rosing-Asvid, A., 2010. Rapid circulation of warm subtropical waters in a major glacial fjord in East Greenland. Nat. Geosci. 3, 182–186.
Thomsen, H.H., Olesen, O.B., 1990. Continued glaciological investigations with respect to hydropower and ice-climate relationships, at Pakitsoq, Jakobshavn, West Greenland. Rapp. Grønl. Geol. Unders. 148, 83–86.
Vieli, A., Nick, F.M., 2011. Understanding and modeling rapid dynamic changes of tidewater outlet glaciers: issues and implications. Surv. Geophys. 32, 437–458.
Wanner, H., Beer, J., Bütikofer, J., Crowley, T.J., Cubasch, U., Flückiger, J., Goosse, H., Grosjean, M., Joos, F., Kaplan, J.O., Küttel, M., Müller, S., Prentice, I.C., Solomina, O., Stocker, T.F., Tarasov, P., Wagner, M., Widmann, M., 2008. Mid- to late Holocene climate change: an overview. Quat. Sci. Rev. 27, 1791–1828.
Wagner, B., Bennike, O., 2012. Chronology of the last deglaciation and Holocene environmental change in the Sisimiut area, south-west Greenland based on lacustrine records. Boreas 41, 481–493.
Wagner, B., Melles, M., Hahne, J., Niessen, F., Hubberten, H.W., 2000. Holocene climate history of Geographical Society O, east Greenland-evidence from lake sediments. Palaeogeogr. Palaeoclimatol. Palaeoecol. 160, 45–68.
Weidick, A., 1992. Jakobshavn Isbræ area during the climatic optimum. Rapp. Grønl. Geol. Unders. 155, 67–72.
Weidick, A., Bennike, O., 2007. Quaternary glaciation history and glaciology of Jakobshavn Isbræ and the Disko Bugt region, West Greenland: a review. Geol. Surv. Den. Greenl. Bull. 14, 78.
Weidick, A., Oerter, H., Reeh, N., Hojmark Thomsen, H., Thorning, L., 1990. The recession of the Inland Ice margin during the Holocene climatic optimum in the Jakobshavn Isfjord area of West Greenland. Palaeogeogr. Palaeoclimatol. Palaeoecol. (Glob. Planet. Change Sect.) 82, 389–399.
Weidick, A., Bennike, O., Citterio, M., Nørgaard-Pedersen, N., 2012. Neoglacial and historical glacier changes around Kangersuneq fjord in southern West Greenland. Geol. Surv. Den. Greenl. Bull. 27, 68.
Young, N.E., Briner, J.P., Stewart, H.A.M., Axford, Y., Csatho, B., Rood, D.H., Finkel, R.C., 2011. Response of the Jakobshavn Isbræ, Greenland, to Holocene climate change. Geology 39, 131–134.